Aggregated dynamic model of active distribution networks for large voltage disturbances

[*]Nuno Fulgêncio[1], Carlos Moreira[1,2], Leonel Carvalho[1], João Peças Lopes[1,2]

nuno.r.fulgencio@inesctec.pt, carlos.moreira@inesctec.pt, leonel.m.carvalho@inesctec.pt, jpl@fe.up.pt
[1]Institute for Systems and Computer Engineering, Technology and Science (INESC TEC)
[2]Faculty of Engineering of the University of Porto (FEUP)

Aggregated dynamic model of active distribution networks for large voltage disturbances

*Nuno Fulgêncio[1], Carlos Moreira[1,2], Leonel Carvalho[1], João Peças Lopes[1,2]

nuno.r.fulgencio@inesctec.pt, carlos.moreira@inesctec.pt, leonel.m.carvalho@inesctec.pt, jpl@fe.up.pt
[1]Institute for Systems and Computer Engineering, Technology and Science (INESC TEC)
[2]Faculty of Engineering of the University of Porto (FEUP)

Abstract— **This paper proposes a "grey-box" aggregated dynamic model for active distribution networks, taking into account a heterogeneous fleet of generation technologies alongside their expected behavior when taking into account the latest European grid codes requirements in terms of voltage support services. The main goal of the proposed model and underlying methodology for its identification is to represent the transient behavior of the active distribution system following large voltage disturbances occurring at the transmission side. The proposed aggregated model is composed by three main components: an equivalent power converter for generation and battery energy storage systems portfolio representation; an equivalent synchronous generation unit; and an equivalent composite load model. The model's parameters are estimated by an evolutionary particle swarm optimization algorithm, by comparing a fully-detailed model of a distribution network with the aggregated model's frequency domain's responses of active and reactive power flows, at the boundary of transmission-distribution interface substation.**

Keywords— **Active distribution networks; Distributed generation; Renewable energy systems; Dynamic modelling.**

1. Introduction

The last decades have been of considerable transformation for electrical power systems, involving a shift from the conventional generation paradigm to the large-scale integration of distributed generation (DG) exploiting Renewable Energy Sources (RES) being connected at all voltage levels, with a significant share being accounted at distribution grids. Alongside, distributed energy resources (DER) are also contributing to change the landscape of future distribution grids, such as the battery energy storage systems (BESS) for supporting the local management of loads and DG, and the need of supplying electric vehicles charging points.

Aiming to assure grid stability and security in face of increasing shares of DG integration, system operators start to require these units to provide network services complementary to the energy production role [1,2]. Taking into account the Continental Europe case [3], specific

requirements have been defined for the connection of generation units to the grid. In particular, generation units have been categorized per type, considering the installed capacity and the voltage level at which they are connected. Even smaller units (in the network code referred to as types A and B), connected to lower voltage levels, are now required to provide frequency sensitive operation modes, namely the capability of active power modulation in case of a grid over-frequency event, and even low voltage fault ride-through (FRT) capabilities. The definition of this set of connection requirements defines a new paradigm for the expected behaviour of the distribution grid itself as well as in what concerns its interaction with the upstream transmission network. Consequently, in future scenarios characterized by increasing shares of RES in the electric power system, the role that DG units connected to the distribution grid have in the overall system performance must be taken into account with respect to different phenomena and operation strategies, once it may represent an important percentage of the total generated power in a given region [4]. Therefore, in order to achieve relevant results within the scope of networks' stability studies, the active distribution networks (ADN) modelling strategies need to be considered.

Within the traditionally approach for assessing system stability from the transmission system operator (TSO) perspective, the distribution networks were modelled as passive lumped loads without specific characterization of dynamic phenomena [5]. The active nature of the distribution grid precludes this approach, requiring new modelling strategies to be properly identified. Given the active nature of distribution networks, modelling of its transient behaviour is becoming of utmost importance for TSO within the scope of system transient stability studies. Nevertheless, confidentiality issues precludes data sharing between distribution and transmission system operators. If the possibility of data sharing is assumed as possible and effective, the complexity of an integrated model accounting for the transmission and distribution grid increases exponentially. To overcome such limitations, it can be envisioned a more active role for DSO regarding the characterization of their grids and connected assets by

providing aggregated models up to the distribution-transmission grid substation while maintaining the privacy of the information. This concept, which supports the applicability of the methodology addressed in this work, is being developed within the framework of the European Union funded project EU-SYSflex [6]. Taking into account large system dominated by synchronous generation units, reduction techniques exploiting modal and coherency-based methods are widely available, but lacking the explicit consideration of DG at the ADNs [7].

Within the aforementioned scope, it is possible to find in the literature some approaches addressing the aggregated modelling of distribution grids with DG [8–11], being that most lean to measurement-based strategies and can be categorized as white-box, black-box and grey-box approaches. White-box strategies require a high level of detail of the system, which is typically not available since distribution networks are very extensive and the complete mathematical characterization of these networks would also represent an increased computational effort; black-box strategies, which may be interesting due to its complete independence of the need for relevant system information, preclude adherence to the relevant phenomena and therefore do not have large acceptance from system operators. Additionally, these solutions are normally highly case-dependent, not being able to represent an extended range of system configurations and operational states (unless, beforehand, considered in the training process). Grey-box strategies may be considered the best suiting approach to this problem, since they exploit a balance between white-box and black-box approaches, while preserving some degree of adherence to the system characteristics. In this case, it is assumed to be known the model structure, being necessary to identify the most adequate parameters it includes. Within this scope it is already possible to find some solutions proposed in the literature. In [5] the authors address the derivation of ADNs aggregated models comprising converter-interfaced generation systems and different types of loads (ZIP-type loads and induction motor based loads). Although the authors consider static and dynamic loads, the generation portfolio is limited to converter-connected units and the adherence to connection requirements such as FRT capability

is not addressed. Also, robustness of the approach regarding different voltage sags at the distribution-transmission interface is also not addressed. In [8], the authors present an equivalency approach for ADNs aiming to address their power-frequency response capabilities; nevertheless, the transient response in face of large voltage disturbances is not considered. In [9] the authors propose an adaptive variable-order transfer function to represent the aggregated response of the ADN, which is a highly case-dependent methodology, not demonstrating robustness to multiple disturbances without model adaption.

In order to overcome some of the limitations identified in the literature, in this paper it is addressed the development of a methodology for the derivation of a robust aggregated model for DG-reach distribution grids considering a wide diversity of inverter-based generation systems (distributed storage units included) being compliant with new grid code requirements such as FRT and reactive current injection capabilities, as well as synchronous based generation systems. The consideration of such a diverse fleet of generation technologies into the equivalent model and the development of a robust aggregated model with respect to a wide range of voltage disturbances is not available in the existing literature, and is an important contribution of this paper. From the load side, static and dynamic load types are considered in the proposed approach, which also enhances the model's diversity and hence the range of its representativeness. The aggregated model is intended to represent the transient behaviour of ADNs in the boundary of the transmission/distribution substation with respect to active and reactive power flows over time, while facing large voltage disturbances resulting from faults occurring in the transmission grid side. Robustness of the proposed solution is addressed by identifying a robust set of parameters capable of covering different distribution grid operating conditions, taking into account different magnitudes of voltage sags at the transmission-distribution interface. The proposed approach assumes a "grey-box" type aggregated equivalent model for which proper parametrization is necessary to be identified. The aggregated model parametrization is based in a meta-heuristic optimization method seeking the best fit of the

aggregated model response to the one derived from the complete distribution grid model. The model structure, parameters estimation and respective test cases are computed recurring to the software tool of MATLAB®, in coordination with the simulation platform of MATLAB/Simulink®.

2. DYNAMIC EQUIVALENT MODEL FOR ADN

For the purpose of this work, the distribution system to be reduced is considered to be operated radially, which typically occurs at the Medium Voltage (MV) level. It is also assumed that the generation system portfolio connected to the distribution grid comprises small synchronous generation units assumed to operate with constant mechanical power, converter-interfaced generation units (such as wind and solar installations) as well as energy storage devices [12]. The system loads are considered to be dynamic (motor-load type) and static (exponential load model). In each model type, different parameter sets available in the literature, for each element, were used in order to create the complete distribution grid model [13–15].

It is also important to point out that, since the emphasis of this study is on the transient behaviour of the voltage, no frequency-dependent events were considered in the vicinity of the transmission-distribution boundary substation where the aggregated response is to be captured from the distribution grid side. Voltage-related transient responses may lead to under-frequency events as a result of the response of converter interfaced units. However, taking into account the typical size of MV-connected generation units, as well as the classification of the generation units in terms of its capacity according to the European Grid Code (according to [3], units from 1 MW up to 50 MW are of type B in the continental Europe, which are required to be sensitive only to over-frequencies), it is reasonable not to consider the frequency response of these units at this stage. Nevertheless, converter interfaced generation systems in the distribution grid side are considered to be FRT-compliant and to be capable of providing dynamic voltage support

during grid faults by means of reactive current injection. Also, the three-phase distribution network is assumed to be balanced.

2.1. Equivalent model structure

Taking into account the fleet of generation systems and loads assumed to be connected to the MV distribution grid, it is proposed to use the generic aggregated model structure depicted in Figure 1, in order to represent the dynamic behavior of the distribution grid at the transmission/distribution HV/MV boundary substation, following transmission grid disturbances. The underlying rationale of the proposed aggregated model is to superimpose the contribution of the elements that contribute dynamically to the behaviour of the overall distribution system. To do so, the model includes three main equivalent components: a composite load, a synchronous generation unit and a power converter accounting for generation and BESS. Each of these components are connected to the transmission/distribution boundary where model aggregation takes place through an equivalent impedance (Z_{Load}, Z_{Gen_1} and Z_{Gen_2}) to emulate voltage drop effects along the distribution grid feeders. The following subsections present in detail each component of the aggregated distribution grid adopted model. The individual models of the components included in the aggregated distribution grid model are of the same type of those considered in the full distribution grid model.
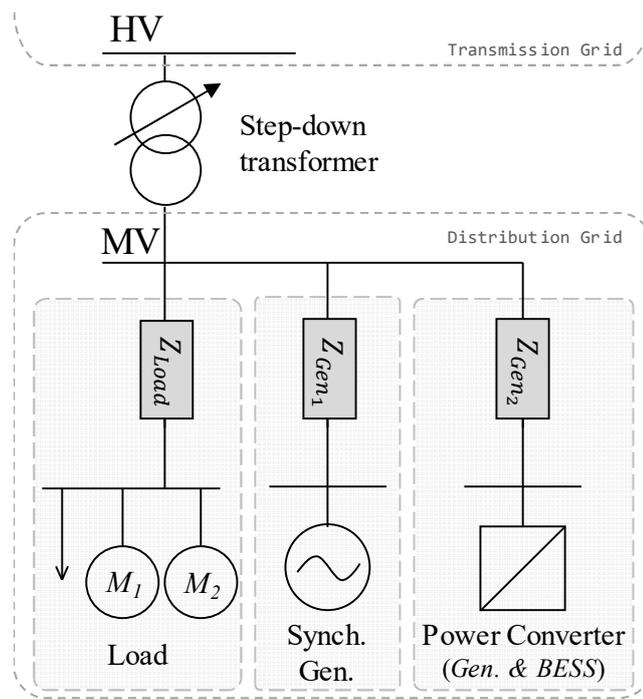
Figure 1 – Aggregated distribution network model structure.

2.1.1. Equivalent load model

The equivalent load model is aggregated into two types, considering one static and two dynamic (motors M_1 and M_2) loads, connected in parallel. The use of this representation is intended to represent the dynamic behaviour of a wide variety of industrial and service sectors' types of loads, covering heating and lighting loads for the static type, and motors for cooling/ventilation, compressed air, refrigeration and industrial appliances for the dynamic type [13,14].

The static load is represented by an exponential model of a dynamic load, where the active and reactive power consumed varies exponentially (with n_p and n_q, respectively) as a function of the voltage, according to the following equations:

$$P(V) = P_0 \left(\frac{V}{V_0}\right)^{n_p} \tag{1}$$

$$Q(V) = Q_0 \left(\frac{V}{V_0}\right)^{n_q} \tag{2}$$

In these functions, P_0 and Q_0 are the initial active and reactive power of the model, and V and V_0 are the measured and initial voltages, respectively.

To represent the dynamic load part, a third order state-of-the-art representation of three-phase asynchronous machines (squirrel cage), modelled in a *dq* rotor reference frame was adopted from the MATLAB/Simulink® library. Motors M_1 and M_2 differ in the respective consideration of constant and rotor-speed dependent torque modes, for a broader representation. Besides their nominal power, each of the motors' models are re-parametrized by adjusting their stator and rotor's resistances and leakage inductances (R_s, L_{l_s}, R_r' and L_{l_r}', in p.u.), as well as the magnetizing inductances (L_m, also in p.u.) and inertia constants (H, in seconds).

2.1.2.   Equivalent synchronous generator model

The representation of the share of synchronous generation units in the aggregated model was achieved through a state-of-the art model of synchronous machine, available in the MATLAB/Simulink® library. The mechanical system is represented by the swing equation, whereas the electrical part is represented by a sixth-order state space model (*dq* reference frame), taking into account the dynamics of the stator, field and damper windings. Available for the equivalent model's parametrization were the machine's nominal power ($S_{n_{synch}}$, in MVA), its inertia constant (H, in seconds), the *d*-axis reactance (X_d), transient reactance (X_d') and sub-transient reactance (X_d'), the *q*-axis reactance (X_q), and sub-transient reactance (X_q''), and finally the leakage reactance (X_l), all in pu. Also the *dq*-frame open-circuit, transient and sub-transient, time constants were available for parametrization (T_{do}', T_{do}'' and T_{qo}'', in seconds). The field voltage of the unit was controlled through the IEEE standard SEXS excitation model. The synchronous units are assumed to operate under constant mechanical power for the duration of the voltage transients under study.

2.1.3.   Equivalent converter model

As a result of the previously depicted conditions considered in this paper, and particularly for the generation portfolio accounted for, the design of the equivalent converter model has been performed in order to accommodate the FRT capability, in line with the most recent grid codes' requirements.

The consideration of converter-connected units in the grid led to the development of a generic equivalent converter, focusing the modelling on the embedded control and the grid-interconnection, while discarding the primary sources' electro- or electro-mechanical interactions. The model is based on a state-of-the-art representation, implemented in the dq reference frame, enabling decoupled control over the active and reactive components of the current. Also, and in line with the most recent grid codes' requirements, the design of the equivalent generation model has been performed in order to accommodate the FRT capability. The block diagram presented in Figure 2 depicts its mathematical implementation, where it is possible to observe the inner current control loops and the outer active and reactive power settings definition.
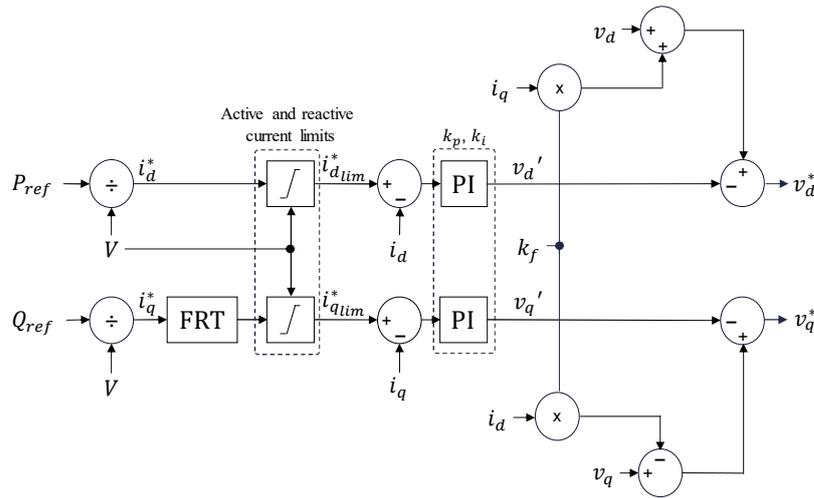
Figure 2 - Equivalent converter model structure.

The inner current control acts separately on the active and reactive components of the current (i_d and i_q) by means of a proportional and integral (PI) control and a feedforward decoupling gain ($k_f = 0.2$). The desired current (i_d^* and i_q^*) is computed according to the power set-points (P_{ref} and Q_{ref}) as a function of the terminal voltage (V). In order to comply with the unit maximum admissible current (i_{max}), the reference current components (i_d^{lim} and i_q^{lim}) are limited according to the rationale presented in the next subsection.

2.1.3.1.   Reactive current injection and FRT capability:

The FRT connection requirement is achieved by assuring the generation unit remains connected to the grid following voltage sags not exceeding a given voltage versus time characteristic curve [3]. In terms of the computational model implementation, it was assumed that converter-interfaced units are FRT-compliant with respect to a fault being cleared in 150 ms.

In addition to the ability of remaining connected during a voltage sag, it is also requested by some system operators that generation units should be capable of providing support to the grid's voltage through reactive current injection as a function of the terminal voltage [16], as depicted in Figure 3. In this case, while maintaining its maximum current (i_{abs}) within limits ($i_{max} = 1$), it is given priority to the reactive current increase, by decreasing the active component, according to the following operation rationale:

If $i_{abs} < i_{max}$

   If $V < V_2$ (see Figure 3)

$$i_q^{lim} = i_q^*, i_q^* \leq i_{max} \tag{3}$$

$$i_d^{lim} = \sqrt{i_{max}^2 - i_q^{*2}} \tag{4}$$

   Else: $i_q^{lim} = i_{max} \sin \theta \; AND \; i_d^{lim} = i_{max} \cos \theta \tag{5}$

Else: $i_q^{lim} = i_{abs} \sin \theta \; AND \; i_d^{lim} = i_{abs} \cos \theta \tag{6}$

With $i_{abs} = \sqrt{i_d^2 + i_q^2}$, and $\theta = \arctan\left(\frac{i_q^*}{i_d^*}\right)$.

The injection of reactive current, upon significant low voltage values in fault operation, is achieved by applying the characteristic curve presented in Figure 3.
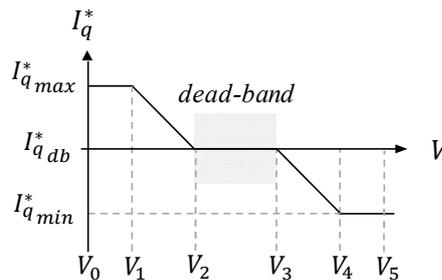
Figure 3 - Voltage to reactive current injection characteristic curve.

2.1.4. Equivalent impedance

The integration of expected voltage drop effects along the distribution feeders was modelled by a π-section line. It was considered one equivalent impedance per each component of the model. The model receives an equivalent resistance, inductance and capacitance (R, L and C), as well as its length. For the parameters' estimation procedure, a typical line resistance per unit of length was defined, together additional factor relating (in percentage) R and L was added (RL_{ratio}).

2.2. Methodological approach for parameters identification

Following the presentation and discussion of the proposed aggregated model structure for the ADN, this section provides the description of the methodological approach for the model's parameters identification regarding the objective to be attained (Figure 4).
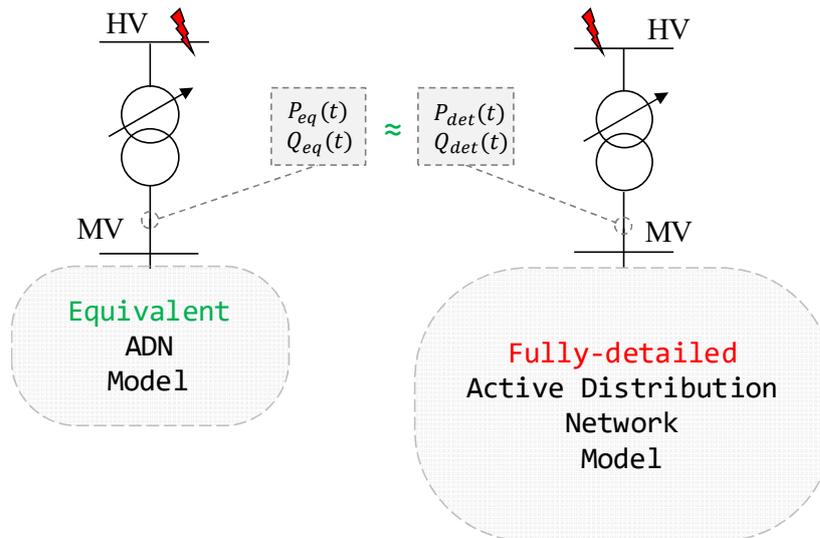
Figure 4 - Schematic for the detailed vs equivalent implemented approach.

Aiming to identify robust parametrizations for the aggregated model, the methodological approach consists on simulating a set of voltage related disturbances on the detailed model of the distribution grid (represented by different voltage sags in the HV bus bar in Figure 4) in order to generate a set of data related to the active and reactive power responses in the HV/MV boundary substation. Then, the same type of voltage disturbances are to be simulated over the aggregated model aiming to best fit the responses obtained in the completed and aggregated models throughout a proper parametrization of the aggregated one (aggregated model training

phase). Afterwards, the model performance is tested with respect to another set of voltage related disturbances not used within the training phase. Besides its representativeness facing trained operational conditions, the model's robustness for cases inter/extrapolation is of upmost importance and is being addressed in this phase by considering the ability of the model to properly response to a set of disturbances with the same set of identified parameters.

The problem formulation associated to the parameter identification in the aggregated distribution grid model can be translated by the following equations, for a number of disturbances under study (nr_{dist}), at the ith disturbance (see Figure 4):

$$\text{Min: } \epsilon_{FFT}(\theta) = \epsilon_{FFT\,P}^2(\theta) + \epsilon_{FFT\,Q}^2(\theta) \tag{7}$$

With:

$$\epsilon_{FFT\,P}(\theta) = \sum_i^{nr_{dist}} P_{eq_{FFT}}(\theta, i) - P_{det_{FFT}}(i) \tag{8}$$

$$\epsilon_{FFT\,Q}(\theta) = \sum_i^{nr_{dist}} Q_{eq_{FFT}}(\theta, i) - Q_{det_{FFT}}(i) \tag{9}$$

Where $P_{eq_{FFT}}(\theta, i)$, $P_{det_{FFT}}(i)$, $Q_{eq_{FFT}}(\theta, i)$ and $Q_{det_{FFT}}(i)$ are the single-sided amplitude spectrums of the Fast Fourier Transforms (FFT) of the normalized signals of the measured active and reactive power for the equivalent and the detailed models, respectively, at a given iteration i and a given set of parameters θ (for the equivalent case).

The FFT is an algorithm that transforms a time-domain signal into a frequency-domain signal, decomposing the original signal into its frequency components – each with a given magnitude and phase. The use of a Fourier transform improves the quantification of the transient dynamics of the signals, enabling an improved assessment and consequent comparison of the signals under study. The active and reactive power FFT errors ($\epsilon_{FFT\,P}(\theta)$, $\epsilon_{FFT\,Q}(\theta)$) compute the total frequency-domain error between the detailed and the aggregated model responses, for a given solution (i.e., a set of parameters) – represented by the state-variables vector (θ) – for all the considered disturbances. Parallel computation was implemented, allowing the allocation of several simulations to different cores.

In order to achieve a good fitting between the response of the two models' responses, the Evolutionary Particle Swarm Optimization (EPSO) method was used to support parameter identification for the aggregated model. EPSO can be seen as a population-based metaheuristic that combines the best features of evolutionary computation and PSO (Particle Swarm Optimization). As an evolutionary method, EPSO includes the standard operators typically found in Genetic Algorithms or Evolutionary Programming. In addition, it contains an ingenious self-adaptive scheme for mutating the strategic parameters (weights) used in the recombination operator, which is borrowed from the PSO's movement equation.

In EPSO, a new solution (X_t) is obtained from the previous solution (X_{t-1}), and the best individual solution (X_b), the best solution found by the population (X_{gb}^*), and the previous velocity (V_{t-1}), are computed according to

$$V_t = w_i^* V_{t-1} + w_m^*(X_b - X_{t-1}) + w_m^* C\left(X_{gb}^* - X_{t-1}\right) \tag{10}$$

$$X_t = X_{t-1} + V_t \tag{11}$$

Where w represents the weights (the subscripts i, m, and c stand for inertia, memory and cooperation of the weights, respectively), C is diagonal matrix of Bernoulli random variables with success probability P, and the superscript * indicates that the corresponding parameter undergoes evolution under a mutation process, which is governed by the mutation rate τ. Note that optimal values for EPSO's parameters can be found using statistical parameter tuning methods [17]. Additional details on EPSO can be found in [18].

The state-variables vector (θ) under identification is composed of 42 parameters (Table 1). These proved to be efficient when adjusting the aggregated model's dynamic transients, as it is shown in the following section, while maintaining the computational time within acceptable limits. The selection of the variables' boundaries followed a trial-and-error approach.

Model	Description	Variable	No. of variables
Load: Static Load (SL)	SL initial active and reactive power margins (*)	$P_{SL_{init\ margin}}$, $Q_{SL_{init\ margin}}$	2
	SL exponents, for load nature definition	n^p, n^q	2
	DL active power margin (*)	$P_{n_{margin}}$	2

Dynamic Loads (DL)	DL *M1*-vs-*M2* ratio	$M1\,M2_{ratio}$	1
	DL resistances and inductances	$R_s, L_{l_s}, R'_r, L_{l_r}{}', L_m$	10
	DL inertia constant	H	2
Eq. Gen. Total	Total installed power margin (*)	$S_{n_{gen\,margin}}$	1
Synchronous Generator	Synchronous over total power ratio	$SynchGen_{ratio}$	1
	Inertia coefficient	H	1
	Reactances	$X_d, X'_d, X''_d, X_q, X''_q$ and X_l	6
	Time constants	T'_{do}, T''_{do} and $T''_{qo},$	3
Power Converter	Initial active and reactive power set-point	P_{ref}, Q_{ref}	2
	Maximum injected reactive current	$I^*_{q_{max}}$	1
Impedances	Equivalent impedances' R/L ratio	RL_{ratio} per impedance	4
	Lines lengths	$LineLength$	4

* percentage of predefined nominal value

Table 1 – Parameters used in the aggregated model fitting.

3. TEST CASE AND RESULTS

A representative schematic of the fully-detailed 72 buses distribution network used for the demonstration of the proposed methodology is presented in Figure 5. The network is operated radially at the MV level (30kV) and considers a total sum of 6.725MVA of load power and 30MVA of installed power from the generation units. Loads are divided into static and dynamic types, considering different parametrizations (as proposed in [13]) for improved diversity, and have been spread randomly throughout the grid. The generation portfolio includes three synchronous units (S_1 to S_3) accounting for a sum of around 15MVA, and eleven converter-connected units (C_1 to C_{11}) representing also a total of around 15MVA, that were also randomly connected to the grid. A 1MVA BESS unit (B_1) is operating at zero-power mode, only for the provision of active and reactive power regulation in faulty operation. Generation units, loads and lines (similarly to the equivalent impedance) are modelled according to what presented in Section 2. The HV network equivalent, upstream to the substation, was modelled as a constant voltage source at the 110kV level, with a 3-phase short-circuit level, at base voltage, of 500MVA, and a X/R ratio of 5. The test system was implemented using the simulation platform of MATLAB®/Simulink®.
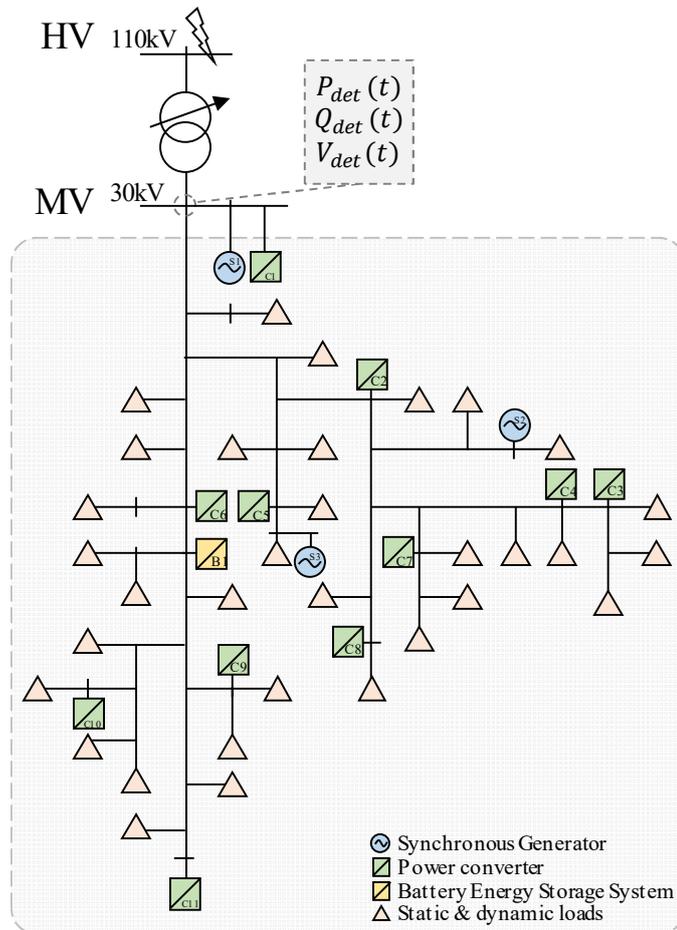
Figure 5 - Fully-detailed distribution network structure.

To characterize the aggregated response of the distribution network and apply the proposed method for aggregated derivation of a distribution grid model, several short-circuits conditions were simulated from the transmission grid side, and the system's dynamic response recorded, at the point of equivalency – downstream to the HV/MV power substation. The faults were considered to have a constant duration of $t_{SC} = 150ms$, before being cleared back to the previous conditions.

Besides the ability of representing a given response on its own, the aggregated model's main advantage is strongly related with the ability of extending its robustness and representativeness upon a range of operational points and disturbances. In line with this rationale, the model was initially trained for a set of short-circuit conditions, that led to voltage sags around 20%, 40%, 60% and 80% of the nominal voltage. The proposed aggregated model was afterwards tested with the resultant set of parameters for another group of disturbances, leading to voltage

decreases to around 30%, 50%, 70% and 90% of the nominal voltage, to assess its performance when applied to untrained conditions. It is important to refer that the training process has considered, as explained in Section 2, the combined error of all the four cases simultaneously. To increase the diversity of the scenarios, the same methodology was applied for two different operation conditions, considering the distribution network importing or exporting active power to the upstream transmission network.

In order to quantify the level of adherence of the aggregated model to the detailed model, a metric based on the normalized standard Euclidean norm of the error was used, expressed in percentage, according the following:

$$accuracy = \left(1 - \frac{\|v_{det} - v_{eq}\|}{\|v_{det}\|}\right)(\%) \tag{12}$$

Where v_{det} and v_{eq} assume the time series responses either for voltage (V_{det}, V_{eq}), active (P_{det}, P_{eq}) and reactive power (Q_{det}, Q_{eq}) for the detailed and the equivalent models.

3.1. Results and outcomes

The results are organized in groups of three plots for each scenario, including the voltage (in pu), active power (in MW) and reactive power (MVar) time series for the period under analysis, for the detailed and the aggregated models, measured at the point of connection with the transmission grid (see Figure 4 and Figure 5). The power flow is considered to be positive when flowing downstream to the power substation, or being imported by the MV distribution network.

In Figure 6 and Figure 7 are depicted the results for the training phase with the distribution network being importing and exporting active power, respectively.
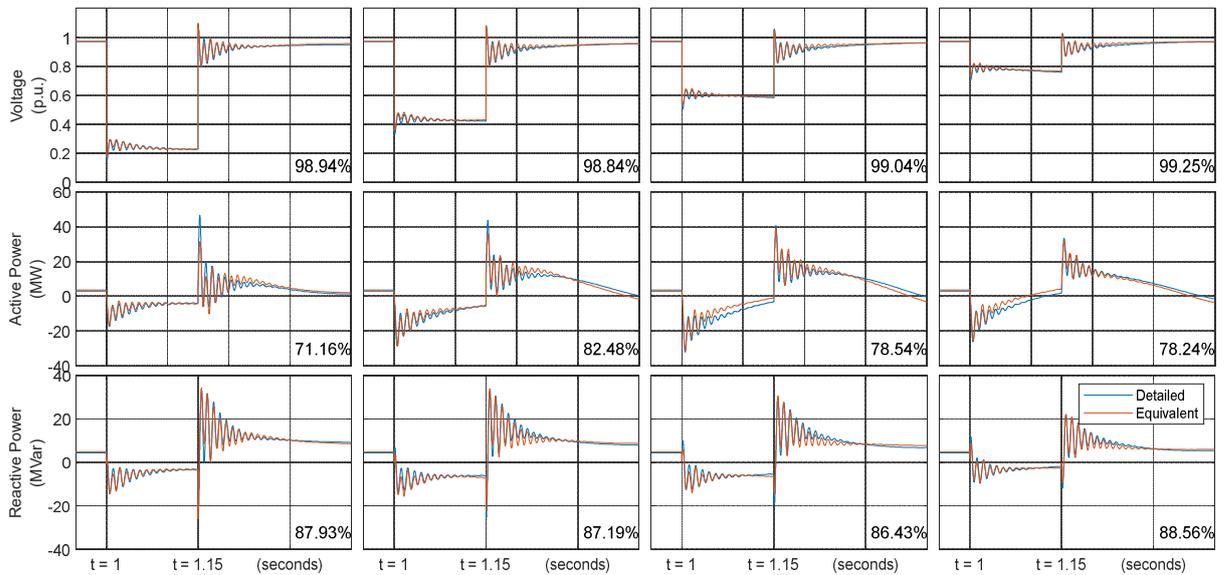
Figure 6 – Model training scenarios for 20%, 40%, 60% and 80% voltage sags, while the distribution network is importing active power (total combined average active and reactive power accuracy 82.18%).
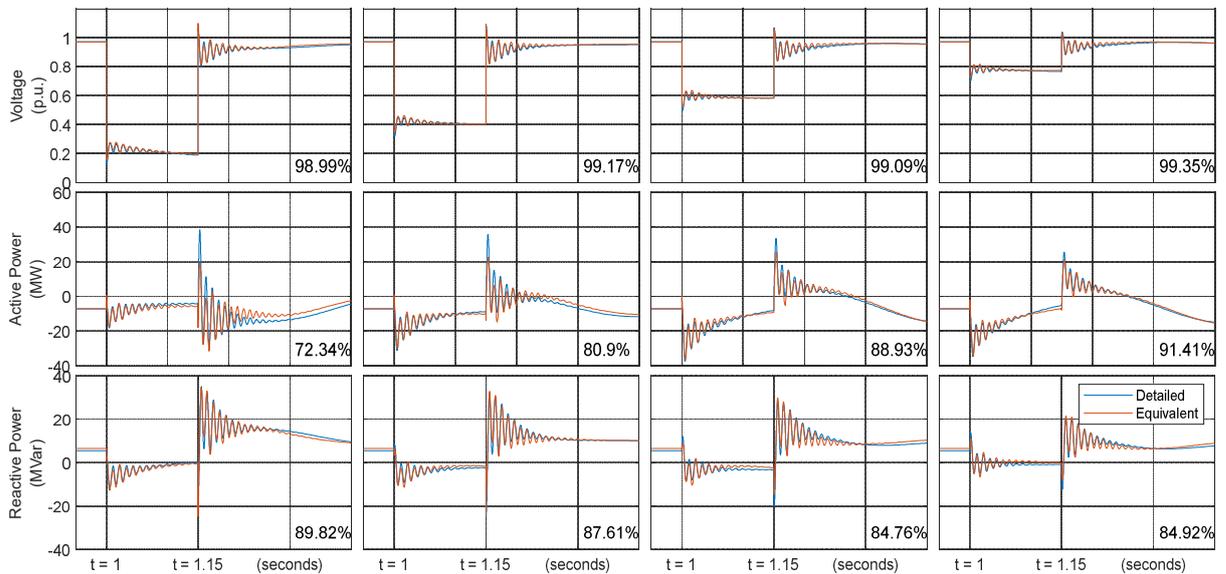
Figure 7 – Model training scenarios for 20%, 40%, 60% and 80% voltage sags, while the distribution network is exporting active power (total combined average active and reactive power accuracy 85.07%).

At this stage, both cases considered 4 voltage-related transient events with different residual voltage magnitudes (20%, 40%, 60% and 80%). These are organized vertically in the figures, and decrease their severity from the left to the right-hand side plots. As expected, voltage responses are very much similar, indicating the testing conditions between detailed and aggregated model are comparable. In both import and export cases, the aggregated model reveals very good fitting when following the fully-detailed model responses. According to the

18

previously presented metric, both cases reveal a high global adherence to the detailed model, with a total combined average of active and reactive power accuracy of 82.18% and 85,07% for the import and export cases, respectively. Active and reactive power responses are able to capture most of the dynamics of the system, considering the immediate response upon the fault and the resultant oscillations, as well as after the fault clearance. Reactive power response presents a higher level of accuracy in both cases, meaning that the estimation process gave priority to the fitting of this component. This is an expected behavior of the model, since at the MV level, with high X/R ratio in the network, voltage is mostly dependent on reactive power flow.

Following the performance evaluation for the aggregated model within the training process, the obtained parametrization of each import/export case was afterwards tested for a set of untrained disturbances, considering the scenarios where voltage drops to 30, 50, 70 and 90% of the nominal value. Figure 8 and Figure 9 illustrate the time series for the voltage, active and reactive responses for these scenarios.
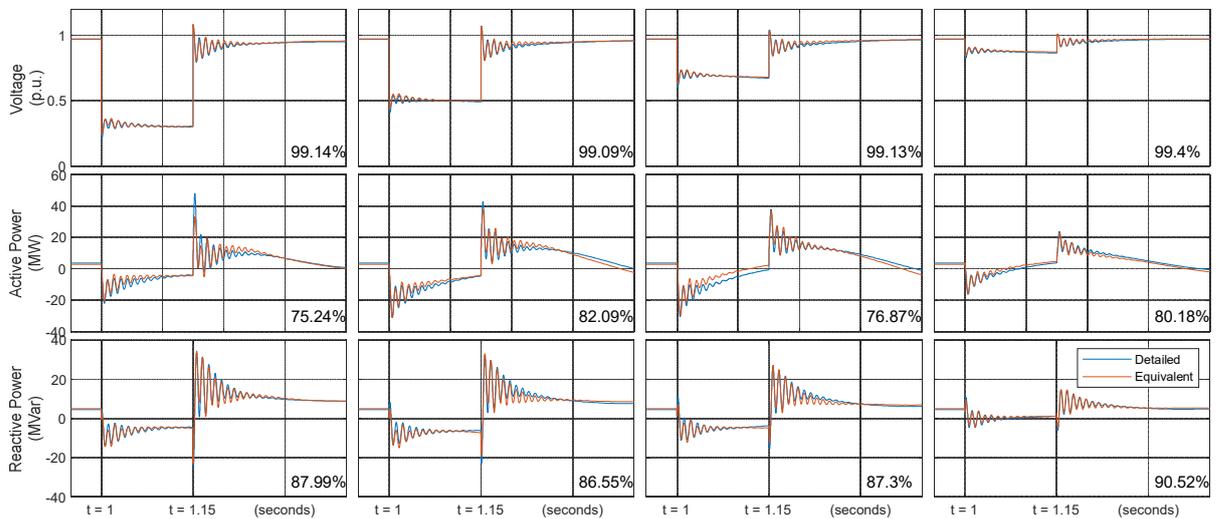
Figure 8 – Model testing scenarios for 30%, 50%, 70% and 90% voltage sags, while the distribution network is importing active power (total combined average active and reactive power accuracy 83.34%).
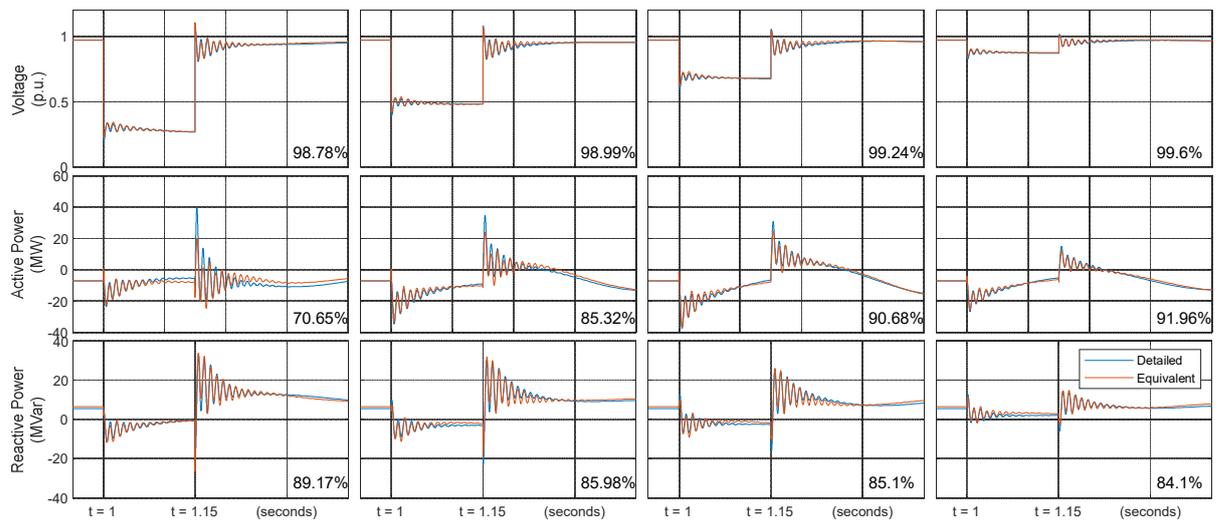
Figure 9 – Model testing scenarios for 30%, 50%, 70% and 90% voltage sags, while the distribution network is exporting active power (total combined average active and reactive power accuracy 85.38%).

The aggregated model seems to be able to satisfactorily follow the same response of the detailed model for both cases, presenting a total combined average of active and reactive power accuracy of 83.34% and 85,38%. The level of adherence of the aggregated model for these untrained conditions is very high, being comparable to the previous trained results. Especially when considering that only one set of parameters is being used for the testing and training phases (per import/export case), the aggregated model response is considered to be very much satisfactory, thus evidencing the robustness of the set of parameters that were identified for the defined case study in face of a relevant set of voltage-related disturbances. The degree of similarity indicates that the model is able to adapt for a wide range of fault severities, and is able to interpolate between them, even for untrained conditions.

4. CONCLUSIONS AND FUTURE WORK

The work presented in this paper proposes and discusses an approach for the development of an aggregated dynamic model for active distribution grids with a heterogeneous fleet of generation resources as well as static and dynamic loads. The generation fleet is composed by a set of synchronous-based generation units as well as FRT-compliant converter-interfaced systems (including the dynamic reactive current injection capability as a function of the voltage sag at the connection point). The proposed aggregated model was compared to a fully-detailed

model for transient voltage-related phenomena occurring in the upstream transmission grid. Throughout a relevant number of case studies, the proposed approach, including the composition/structure of the aggregated model and a single set of parameters covering trained and untrained scenarios, demonstrated to be very effective and robust with respect to the magnitude of the voltage-related transients, revealing high levels of adherence to the detailed model's active and reactive power responses.

Within the scope and relevance of ADN transient and dynamic response characterization, next steps for future work include the extension of the size and complexity of the cases under study, including not only medium voltage radial networks, but also high voltage, meshed networks, since in some countries it belongs also to the domain of distribution system operators. Revisiting the structure of the equivalent model and comparing of the proposed optimization method with others available in the literature is also intended to be included in future development. Moreover, the non-linear nature resulting from the risk of tripping of the non- fault ride-through compliant generation units following a voltage sag, needs to be addressed. Also, it is of high relevance to account for a wider range of distribution grid operational scenarios, and extract relevant information aiming to establish comprehensive relations regarding the potential impact on the equivalent model parametrization.

The availability and need of this type of models is becoming of fundamental importance given the highly distributed nature of the future power system generation portfolio, as well as the expected role each generation asset will play in face of the increasing connection requirements that are being demanded. Such modelling approach is of utmost importance for further supporting the interoperability between the transmission and distribution system operators.

REFERENCES

[1]   F. Díaz-González, M. Hau, A. Sumper, O. Gomis-Bellmunt, Participation of wind power plants in system frequency control: Review of grid code requirements and control methods, Renew. Sustain. Energy Rev. 34 (2014) 551–564. doi:10.1016/J.RSER.2014.03.040.

[2]   A.B. Attya, J.L. Dominguez-Garcia, O. Anaya-Lara, A review on frequency support provision by wind power plants: Current and future challenges, Renew. Sustain. Energy Rev. 81 (2018) 2071–2087. doi:10.1016/J.RSER.2017.06.016.

[3]   European Commission, Establishing a network code on requirements for grid connection of generators, 2016.

[4]   N. Hatziargyriou, T. Van Cutsem, J. Milanovic, P. Pourbeik, C. Vournas, O. Vlachokyriakou, P. Kotsampopoulos, M. Hong, R. Ramos, J. Boemer, P. Aristidou, V. Singhvi, J. dos Santos, L. Colombari, Contribution to Bulk System Control and Stability by Distributed Energy Resources connected at Distribution Network, IEEE PES Technical Report PES-TR 22, (2017).

[5]   S. Mat Zali, J. V. Milanovic, Generic model of active distribution network for large power system stability studies, IEEE Trans. Power Syst. 28 (2013) 3126–3133. doi:10.1109/TPWRS.2012.2233223.

[6]   EU-SysFlex Project, (n.d.). http://eu-sysflex.com/ (accessed July 10, 2019).

[7]   U.D. Annakkage, N.K.C.C. Nair, Y. Liang, A.M. Gole, V. Dinavahi, B. Gustavsen, T. Noda, H. Ghasemi, A. Monti, M. Matar, R. Iravani, J.A. Martinez, Dynamic system equivalents: A survey of available techniques, IEEE Trans. Power Deliv. 27 (2012) 411–420. doi:10.1109/TPWRD.2011.2167351.

[8]   H. Golpîra, H. Seifi, M.R. Haghifam, Dynamic equivalencing of an active distribution network for large-scale power system frequency stability studies, IET Gener. Transm. Distrib. 9 (2015) 2245–2254. doi:10.1049/iet-gtd.2015.0484.

[9]   E.O. Kontis, S.P. Dimitrakopoulos, A.I. Chrysochos, G.K. Papagiannis, T.A. Papadopoulos, Dynamic equivalencing of active distribution grids, 2017 IEEE Manchester PowerTech, Powertech 2017. (2017). doi:10.1109/PTC.2017.7981103.

[10]   F.O. Resende, J. Matevosyan, J. V. Milanovic, C. Wg, Application of dynamic equivalence techniques to derive aggregated models of active distribution network cells and microgrids, 2013 IEEE Grenoble Conf. PowerTech, POWERTECH 2013. (2013) 1–6. doi:10.1109/PTC.2013.6652356.

[11]   V. Miranda, H. Hrvoje, Á. Jaramillo Duque, Stochastic Star Communication Topology in Evolutionary Particle Swarms (EPSO), Int. J. Comput. Intell. Res. 4 (2008) 105–116. doi:10.5019/j.ijcir.2008.130.

[12]   Joint Working Group C4/C6.35/CIRED, Modelling of Inverter- Based Generation for Power System Dynamic Studies, 2018.

[13]   Di. Chakravorty, B. Chaudhuri, S.Y.R. Hui, Rapid Frequency Response from Smart Loads in Great Britain Power System, IEEE Trans. Smart Grid. 8 (2017) 2160–2169. doi:10.1109/TSG.2016.2517409.

[14]   A. Gaikwad, P. Markham, P. Pourbeik, Implementation of the WECC Composite Load Model for utilities using the component-based modeling approach, Proc. IEEE Power Eng. Soc. Transm. Distrib. Conf. 2016-July (2016) 0–4. doi:10.1109/TDC.2016.7520081.

[15]   J. V Milanovi, K. Yamashita, S.M. Villanueva, S.Ž. Djoki, S. Member, L.M. Korunovi, International Industry Practice on Power System Load Modeling, 28 (2013) 3038–3046.

[16]   A. Etxegarai, P. Eguia, E. Torres, G. Buigues, A. Iturregi, Current procedures and practices on grid code compliance verification of renewable power generation, Renew. Sustain. Energy Rev. 71 (2017) 191–202. doi:10.1016/J.RSER.2016.12.051.

[17]   L.M. Carvalho, F. Loureiro, J. Sumaili, H. Keko, V. Miranda, C.G. Marcelino, E.F. Wanner, Statistical tuning of DEEPSO soft constraints in the Security Constrained Optimal Power Flow problem, in: 2015 18th Int. Conf. Intell. Syst. Appl. to Power Syst., IEEE, 2015: pp. 1–7. doi:10.1109/ISAP.2015.7325576.

[18]   V. Miranda, N. Fonseca, EPSO - best-of-two-worlds meta-heuristic applied to power system problems, in: Proc. 2002 Congr. Evol. Comput. CEC'02 (Cat. No.02TH8600), IEEE, 2002: pp. 1080–1085. doi:10.1109/CEC.2002.1004393.

[19]   A.G. Madureira, J.A. Peças Lopes, Coordinated voltage support in distribution networks with distributed generation and microgrids, IET Renew. Power Gener. 3 (2009) 439. doi:10.1049/iet-rpg.2008.0064.

LIST OF FIGURES

LIST OF TABLES

In this section it is included supplementary information on the network characterization, including detailed data of generation units and loads for the detailed case, as well as the resultant parametrization of the equivalent model for the presented test cases, in Section 3. For further information, a detailed characterization of the distribution network used in the same section can be found in [19].

The following tables depict further details on the generation units connected to the distribution network under reduction.

Name	Type	Nominal Power (MW)	Initial Active Power (pu)	Initial Reactive Power (pu)
G1 - G10	IBG	1	Random between 0.4 and 0.6	Random between 0.05 and 0.15
G11	IBG	5	0.5	0.1
B1	BESS	1	0	0

Table 2 – Converted-connected generation and storage characteristics summary (IGB – Inverter-based generation; BESS – Battery Energy Storage System).

Max. reactive current, Iq_{max} (pu)	Dead-band reactive current, Iq_{db} (pu)	Minimum reactive current, Iq_{min} (pu)	Voltage steps (V)					
			V0	V1	V2	V3	V4	V5
1	0	-1	0	0,05	0,95	1,25	1,95	2

Table 3 – Voltage-to-reactive-current characteristic of the converter-connected units, under fault ride through operation (Figure 3).

Name	Nominal Power (MW)	Reactances (pu)						Time constants (s)			Stator Resistance (pu)	Inertia Constant (s)
		X_d	X_d'	X_d''	X_q	X_q''	X_l	T_{do}'	T_{do}''	T_{qo}''	R_s	H
S1	10,625	1,68	0,23	0,17	0,85	0,35	0,12	6	0,06	0,08	~0,003	1,5
S2	2	2,3	0,43	0,215	1,32	0,15	0,12	5,8	0,025	0,05	~0,004	1,714
S3	2	2,3	0,43	0,215	1,32	0,15	0,12	5,8	0,025	0,05	~0,004	1,714

Table 4 – Synchronous generators' electrical characteristics.

Loads modelling has considered a static and a dynamic part. The following tables present the different sets of parameters regarding each part, randomly assigned to every load considered in the detailed network case.

Type	Power Factor	n_p	n_q
1	1	1,95	0
2	1	2	0
3	0,9	1	3

Table 5 – Types and the corresponding parameters used for the static part of the loads.

Type	Stator resistance and reactance (pu)		Magnetizing Reactance (pu)	Rator resistance and reactance (pu)		Inertia constant (s)
	Rs	Lls	Lm	Rr	Llr	H
1	0,031	0,1	3,2	0,018	0,18	0,7
2	0,013	0,067	3,8	0,009	0,17	1,5
3	0,053	0,083	1,9	0,036	0,068	0,28
4	0,013	0,067	3,8	0,009	0,17	1,5

Table 6 – Types and the corresponding parameters used for the dynamic part of the loads.

Load No.	Installed Capacity (kW)	Static Load type (see Table 5)	Dynamic Load type (see Table 6)
1	50	1	1
2	50	2	2
3	100	1	3
4	100	2	4
5	100	3	3
6	100	3	1
7	50	1	2
8	100	3	3
9	1200	2	4
10	100	1	2
11	630	1	1
12	25	2	2
13	160	3	3
14	100	2	4
15	160	1	1
16	160	3	2
17	50	3	3
18	100	2	4
19	250	1	3
20	50	2	1
21	100	2	2
22	50	1	3
23	100	2	4
24	100	1	1
25	1335	3	2
26	100	1	3
27	630	1	1
28	100	3	4
29	100	2	4
30	25	2	2
31	250	2	3
32	100	3	1
33	100	1	2

Table 7 – Loads characterization per type.

Additionally, a ratio between static and dynamic parts was also assigned randomly to each of the loads. The total installed capacity reflects the sum of these two parts.

Moreover, and in order to ensure the test cases replicability, the parametrization of the equivalent model for both the import and export cases is following depicted.

Model	Description	Variable	Parameters Values			Unit
			Min	Identified Value	Max	
Static Load (SL)	SL initial active and reactive power margins (*)	$P_{SL_{init\ margin}}$	0,9	1,082	1,1	n/a
		$Q_{SL_{init\ margin}}$	0,9	0,909	1,1	n/a
	SL exponents, for load nature definition	n^p	0,1	0,787	2,1	n/a
		n^q	0	1,873	3,1	n/a
Dynamic Loads (DL)	DL1 active power margin (*)	$P_{n1_{margin}}$	0,9	1,077	1,1	n/a
	DL $M1$-vs-$M2$ ratio	$M1/M2_{ratio}$	0,4	0,571	0,6	n/a
	DL1 resistances and inductances	$R1_s$	0,029	0,031	0,032	p.u.
		$L1_{l_s}$	0,09	0,107	0,11	p.u.
		$L1_m$	3,1	3,216	3,3	p.u.
		$R1'_r$	0,015	0,018	0,02	p.u.
		$L1_{l_r}{}'$	0,01	0,182	0,2	p.u.
	DL1 inertia constant	H_{M1}	0,6	0,733	0,8	s
	DL2 active power margin (*)	$P_{n2_{margin}}$	0,9	1,064	1,1	s
	DL2 resistances and inductances	$R2_s$	0,029	0,031	0,032	p.u.
		$L2_{l_s}$	0,09	0,091	0,11	p.u.
		$L2_m$	3,1	3,267	3,3	p.u.
		$R2'_r$	0,015	0,016	0,02	p.u.
		$L2_{l_r}{}'$	0,01	0,042	0,2	p.u.
	DL2 inertia constant	H_{M2}	0,6	0,795	0,8	s
Eq. Gen. Total	Total installed power margin (*)	$S_{n_{gen\ margin}}$	0,8	0,860	1,2	n/a
Synchronous Generator	Synchronous over total power ratio	$SynchGen_{ratio}$	0,01	0,375	0,99	n/a
	Reactances	X_d	1,176	1,480	2,184	p.u.
		X'_d	0,161	0,199	0,299	p.u.
		X''_d	0,119	0,145	0,221	p.u.
		X_q	0,595	0,874	1,105	p.u.
		X''_q	0,245	0,318	0,455	p.u.
		X_l	0,084	0,120	0,156	p.u.
	Time constants	T'_{do}	4,2	7,199	7,8	s
		T''_{do}	0,042	0,077	0,078	s
		T''_{qo}	0,056	0,089	0,104	s
	Inertia coefficient	H	1,3	1,680	3	s
Power Converter	Initial active and reactive power set-point	P_{ref}	0,1	0,281	1,1	p.u.
		Q_{ref}	0,01	0,089	0,9	p.u.
	Maximum injected reactive current	$I^*_{q_{max}}$	0,7	1,164	2,5	p.u.
Impedances	Equivalent impedances' R/L ratio	$sync_{RL_{ratio}}$	0,3	0,463	0,8	n/a
		$conv_{RL_{ratio}}$	0,3	0,462	0,8	n/a
		$load_{RL_{ratio}}$	0,3	0,377	0,8	n/a
		$storage_{RL_{ratio}}$	0,3	0,486	0,8	n/a
	Lines lengths	$sync_{LineLength}$	0,8	0,840	1,2	m
		$conv_{LineLength}$	0,8	0,856	1,2	m

| | | $load_{LineLength}$ | 0,8 | 1,164 | 1,2 | m |
| | | $storage_{LineLength}$ | 0,8 | 0,888 | 1,2 | m |

Table 8 – Equivalent model's identified parameters for the case presented in Figure 6 and Figure 8, while the active distribution network is importing active power.

| Model | Description | Variable | Parameters Values | | | Unit |
			Min	Identified Value	Max	
Static Load (SL)	SL initial active and reactive power margins (*)	$P_{SL_{init\ margin}}$	0,9	0,900	1,1	n/a
		$Q_{SL_{init\ margin}}$	0,9	1,043	1,1	n/a
	SL exponents, for load nature definition	n^p	0,1	2,095	2,1	n/a
		n^q	0	3,099	3,1	n/a
Dynamic Loads (DL)	DL1 active power margin (*)	$P_{n1_{margin}}$	0,9	1,094	1,1	n/a
	DL $M1$-vs-$M2$ ratio	$M1/M2_{ratio}$	0,4	0,578	0,6	n/a
	DL1 resistances and inductances	$R1_s$	0,029	0,030	0,032	p.u.
		$L1_{l_s}$	0,09	0,109	0,11	p.u.
		$L1_m$	3,1	3,265	3,3	p.u.
		$R1'_r$	0,015	0,015	0,02	p.u.
		$L1_{l_r}{}'$	0,01	0,176	0,2	p.u.
	DL1 inertia constant	H_{M1}	0,6	0,800	0,8	s
	DL2 active power margin (*)	$P_{n2_{margin}}$	0,9	0,964	1,1	s
	DL2 resistances and inductances	$R2_s$	0,029	0,032	0,032	p.u.
		$L2_{l_s}$	0,09	0,091	0,11	p.u.
		$L2_m$	3,1	3,264	3,3	p.u.
		$R2'_r$	0,015	0,016	0,02	p.u.
		$L2_{l_r}{}'$	0,01	0,050	0,2	p.u.
	DL2 inertia constant	H_{M2}	0,6	0,694	0,8	s
Eq. Gen. Total	Total installed power margin (*)	$S_{n_{gen\ margin}}$	0,8	0,861	1,2	n/a
Synchronous Generator	Synchronous over total power ratio	$SynchGen_{ratio}$	0,01	0,564	0,99	n/a
	Reactances	X_d	1,176	1,604	2,184	p.u.
		X'_d	0,161	0,297	0,299	p.u.
		X''_d	0,119	0,221	0,221	p.u.
		X_q	0,595	0,752	1,105	p.u.
		X''_q	0,245	0,454	0,455	p.u.
		X_l	0,084	0,112	0,156	p.u.
	Time constants	T'_{do}	4,2	4,499	7,8	s
		T''_{do}	0,042	0,076	0,078	s
		T''_{qo}	0,056	0,080	0,104	s
	Inertia coefficient	H	1,3	1,301	3	s
Power Converter	Initial active and reactive power set-point	P_{ref}	0,1	0,813	1,1	p.u.
		Q_{ref}	0,01	0,053	0,9	p.u.
	Maximum injected reactive current	$I^*_{q_{max}}$	0,7	0,784	2,5	p.u.
Impedances	Equivalent impedances' R/L ratio	$sync_{RL_{ratio}}$	0,3	0,562	0,8	n/a
		$conv_{RL_{ratio}}$	0,3	0,546	0,8	n/a
		$load_{RL_{ratio}}$	0,3	0,513	0,8	n/a
		$storage_{RL_{ratio}}$	0,3	0,398	0,8	n/a
	Lines lengths	$sync_{LineLength}$	0,8	0,802	1,2	m
		$conv_{LineLength}$	0,8	0,853	1,2	m

| | | $load_{LineLength}$ | 0,8 | 1,083 | 1,2 | m |
| | | $storage_{LineLength}$ | 0,8 | 0,989 | 1,2 | m |

Table 9 – Equivalent model's identified parameters for the case presented in Figure 7 and Figure 9, while the active distribution network is exporting active power.